

Synthesis of the integral sliding mode control and the robust internal-loop compensator for a class of nonlinear systems with matched uncertainties

Almir Salihbegovic, Mujo Hebibovic and Emir Sokic
Department for Automatic Control and Electronics
Faculty of Electrical Engineering, University of Sarajevo
71000 Sarajevo, Bosnia and Herzegovina
almir.salihbegovic@etf.unsa.ba

Abstract—This paper presents the design procedure of the integral sliding mode controller with enhanced robustness properties for a class of nonlinear uncertain systems. The integral sliding mode control (I-SMC) is synthesized with the generalized disturbance attenuation scheme called robust internal-loop compensator (RIC) through the Lyapunov redesign framework, thus introducing a generalisation of the well-known case for linear systems. The resulted two-layer control structure employs the classical controller with the feedforward term in the outer control loop to track the reference, while the inner control loop compensates the generalized disturbance and provides robust stability. The closed-loop system is proved to be asymptotically stable via Lyapunov stability theory. The developed control algorithm is used for attitude tracking of the small-scale helicopter system in the presence of additional parametric uncertainties and external disturbances. An excellent tracking performance and robustness stability of the proposed control method are revealed through computer simulations and experimental testing over the whole domain of the helicopter outputs.

Index Terms—Sliding mode control, robust internal-loop compensator, disturbance observer, robust stability, Lyapunov methods, asymptotic stability, attitude control, laboratory helicopter.

I. INTRODUCTION

A robust control design procedure for a nonlinear uncertain system includes two important requirements: performance specification of the closed-loop system and robustness to the modelling uncertainties, external and internal disturbances. A quantified trade-off between these two desired requirements has been provided using the generalised disturbance attenuation framework, called robust internal-loop compensator (RIC) [1]–[5]. Although effective performances and unified analysis of the model based disturbance compensation algorithms have been achieved, the concepts of RIC are only presented for the linear systems.

Small-scale helicopters are highly nonlinear systems with significant cross-couplings, unpredictable inputs (disturbance and noise), unknown dynamics, inherently unstable characteristics and parametric uncertainties. In general, small-scale helicopters are versatile flying machines, capable to perform complex manoeuvres and low altitude flights. Therefore, they have been successfully used in various applications, such as search and rescue operations, inspection in inaccessible

areas and emergency situations like nuclear disasters, floods, etc. On the other hand, small-scale helicopters are more susceptible to wind gusts and physical parameters variation than their full sized counterparts due to the light-weighted structure.

In the recent decades different control techniques have been intensively developed to address the autonomous flight of aerial vehicles [6]–[8]. Various control algorithms [9]–[11], such as classical proportional-integral-derivative (PID) controller, linear quadratic optimal control combined with a state estimator (LQG), optimal linear quadratic output control (PLQ), model predictive control (MPC) and fuzzy control, have already been implemented to the laboratory small-scale helicopter system CE 150 supplied by Humosoft. The addressed algorithms do not consider estimation of disturbances, uncertainties and cross-coupling dynamics, thus tracking performances are slightly degraded. Significantly improved tracking performances and decreased power consumption of the small-scale helicopter CE 150 are presented in [12] using the disturbance observer (DOB) based control. Furthermore, our previous paper [13] describes the disturbance observer based sliding mode control (SMC) of the helicopter system CE 150 in the presence of additional parametric uncertainties and external disturbances, which are main difficulties for the motion control.

This paper introduces a generalisation of the RIC scheme for a class of linear systems, by synthesis of the nonlinear I-SMC and the linear RIC for a class of nonlinear uncertain systems through Lyapunov redesign framework. The new control term based on the RIC is introduced to improve robustness properties of the closed-loop system and reduce chattering effect of the I-SMC. In order to enhance the performances of the DOB based SMC algorithm described in [13], the proposed approach in this paper provides a systematic way to tune the controller parameters for robust stability and performance specification using the RIC [1]–[5]. This resulted in a higher control bandwidth of the closed-loop system, which is very important for small-scale helicopters with fast dynamics, especially during aggressive flights. First, the classical controller with the feedforward control term is developed based on the nominal model. Then the RIC based control term is proposed in order to

compensate plant input generalised disturbances, and the I-SMC term is introduced to provide finite time convergence to the equilibrium solution and robustness to the disturbance compensation error. Additional disturbances in the form of wind gusts and 30% uncertainties on the model parameters are applied to the small-scale helicopter system CE 150 as in [13] to demonstrate the control quality. Differently from the previous papers [9]–[13], dynamic changes in the helicopter center of gravity are provided by moving the ballast along its own horizontal axis using the servomechanism. Excellent tracking performances of the proposed control structure will be shown through both, simulation and real experiment, even in the presence of these additional disturbances.

The paper is organized as follows. Synthesis of the I-SMC and the RIC for a class of nonlinear uncertain systems is introduced in Section II using the Lyapunov redesign framework. In Section III the helicopter model and control strategy are presented. Simulation and experimental results are discussed in Section IV. Concluding remarks are given in Section V.

II. SYNTHESIS OF THE I-SMC AND THE RIC IN THE LYAPUNOV REDESIGN FRAMEWORK

This section presents synthesis of the I-SMC and the RIC through the Lyapunov redesign framework for a class of nonlinear uncertain systems. Without loss of generality, the proposed control method is presented for SISO systems, which provide common insight about the basic concepts of the robust motion controller design.

Consider a single degree of freedom mechanical system (either translational or rotational) [14], [15]:

$$a(q)\ddot{q}(t) + \tau_d(t, q, \dot{q}, \tau) = \tau(t, q, \dot{q}), \quad (1)$$

where $q(t)$ and $\dot{q}(t)$ represent the state variables, position and velocity, respectively, $\tau(t, q, \dot{q})$ denotes the control input, $a(q)$ is continuous strictly positive function representing inertia of the system, and $\tau_d(t, q, \dot{q}, \tau)$ denotes the plant input disturbance which includes Coriolis and friction torques, gravitational torque and external disturbances. The functions $a(q)$ and $\tau_d(t, q, \dot{q}, \tau)$ are defined for $(t, q, \dot{q}, \tau) \in [0, \infty) \times D \times D \times D$, where $D \subset \mathbb{R}$ is a domain that contains the origin. Assume that τ_d is piecewise continuous in t and locally Lipschitz in q, \dot{q} and τ , so that with the feedback control τ , that is piecewise continuous in t and locally Lipschitz in q and \dot{q} , the closed-loop system will have a unique solution through every point $(t_0, q_0, \dot{q}_0) \in [0, \infty) \times D \times D$. The acceleration $\ddot{q}(t)$ is also assumed to be continuous and bounded function. The torque $\Delta a(q)\ddot{q}$ induced by varying inertia $\Delta a(q) = a(q) - a_n$ can be lumped into the generalized plant input disturbance $\tau_{dis} = \tau_d + \Delta a(q)\ddot{q}$ if the nominal inertia coefficient a_n is known, so the perturbed system is described with (2):

$$a_n\ddot{q}(t) + \tau_{dis}(t, q, \dot{q}, \tau) = \tau(t, q, \dot{q}). \quad (2)$$

The plant input generalized disturbance τ_{dis} may additionally include various uncertain terms due to the model simplification, parameter uncertainties, etc. The uncertain torque

τ_{dis} satisfies an important structural property called matching condition. Namely, disturbance term τ_{dis} and control input τ enters the system (2) at the same point.

The tracking error $e(t, q)$ is defined as difference between the actual output $q(t)$ and the reference input $q_{ref}(t)$:

$$e(t, q) = q(t) - q_{ref}(t), \quad (3)$$

where the reference input to the controlled plant q_{ref} is assumed continuous and differentiable function for an appropriate number of times. The control law will be designed so the system output q is forced to satisfy $e(t, q) = 0$ in equilibrium. In other words, the system output should be constrained to the domain or manifold:

$$S_1 = \{q \mid e(t, q) = 0\}. \quad (4)$$

The generalized error $\sigma(t, q, \dot{q})$ is introduced in order to provide relative degree one ($r = 1$) with respect to the control input τ :

$$\sigma(t, q, \dot{q}) = \dot{e}(t, q) + \Lambda_1 e(t, q) + \Lambda \int_0^t e(t, q) dt, \quad (5)$$

where Λ and Λ_1 are positive constants. Due to the steady state error attenuation, an integral component of the tracking error (3) is included in the generalized error (5). The control objective can be reformulated using the generalized error σ to drive the system output into the integral sliding manifold:

$$S_2 = \{q \mid \sigma(t, q, \dot{q}) = 0\}. \quad (6)$$

Let us choose the nominal model of the system (2) as:

$$a_n\ddot{q}_n = \tau_n, \quad (7)$$

where q_n is the nominal output generated internally by the nominal control input τ_n . We proceed to design a stabilizing controller using this nominal model. The generalized error dynamics of the nominal system is computed using (5) and (7):

$$\dot{\sigma} = a_n^{-1}\tau_n - (\ddot{q}_{ref} - 2\Lambda\dot{e} - \Lambda^2 e). \quad (8)$$

The equivalent control is chosen to cancel right-hand side of (8):

$$\tau_n^{eq} = a_n (\ddot{q}_{ref} - 2\Lambda\dot{e} - \Lambda^2 e). \quad (9)$$

Implementation of the equivalent control (9) is presented in Fig. 1, where $P_n(s) = (a_n s^2)^{-1}$ is the transfer function of the nominal system, $C_{ff}(s) = a_n s^2$ and $C(s) = a_n (2\Lambda s + \Lambda^2) e$ represent the transfer functions of the feedforward and the feedback controller, respectively. The feedforward control $C_{ff}(s)$ denotes nominal plant inverse, thus it enhances tracking performance and minimizes the transfer function:

$$\frac{e(s)}{q_{ref}(s)} = \frac{P_n(s)C_{ff}(s) - 1}{1 - P_n(s)C(s)}. \quad (10)$$

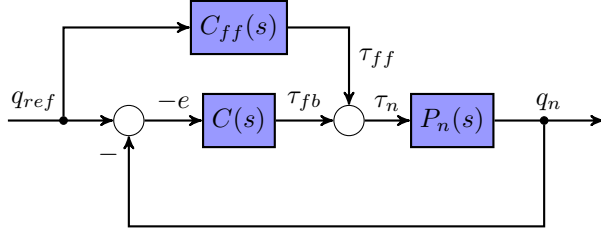


Fig. 1. Standard nominal control structure

Since the feedforward control $C_{ff}(s)$ does not affect closed loop stability, the transfer function from the reference input q_{ref} to the nominal output q_n can be arranged from Fig. 1:

$$\frac{q_n(s)}{q_{ref}(s)} = \frac{\Lambda(2s + \Lambda)s}{s^2 + 2\Lambda s + \Lambda^2}. \quad (11)$$

The transfer function (11) has two poles in the left half-plane, so the feedback control $C(s)$ stabilizes the nominal closed loop system.

Suppose now that the system (2) is affected with uncertainties τ_{dis} and apply the control (12):

$$\tau(t, q, \dot{q}) = \tau_n^{eq}(t, q, \dot{q}) + \tau_v(t, q, \dot{q}) + \hat{\tau}_{dis}(t, q, \dot{q}) \quad (12)$$

to the nominal system (7). The resulting closed-loop system:

$$a_n \ddot{q} = \tau_n^{eq} + \tau_v + \hat{\tau}_{dis} - \tau_{dis}, \quad (13)$$

is a perturbation of the nominal closed-loop system (7). The block structure of the system (13) is depicted in Fig. 2. Here, $\tau_v(t, q, \dot{q})$ and $\hat{\tau}_{dis}(t, q, \dot{q})$ represent the additional feedback controls, which need to be designed in such a way that the overall control (12) stabilizes the actual system (13) in the presence of internal and external disturbances. The additional control $\hat{\tau}_{dis}$ is introduced in order to compensate the plant input generalized disturbance τ_{dis} . The additional control τ_v is included in the overall control (12) to provide sliding mode motion toward the manifold (6) and enhancement of disturbance attenuation characteristic. In complex domain, the disturbance compensation error is expressed as:

$$p(\tau_{dis}, Q) = \tau_{dis} - \hat{\tau}_{dis} = (1 - Q)\tau_{dis}, \quad (14)$$

where the disturbance observer dynamics $\hat{\tau}_{dis} = Q(s)\tau_{dis}$ is described with the linear filter low-pass $Q(s)$. The disturbance estimation error p can be treated as the input disturbance in (13):

$$a_n \ddot{q} = \tau_n^{eq} + \tau_v - p, \quad (15)$$

so the additional control τ_v should achieve robustness to the disturbance compensation error p , rather than provide compensation of the plant input generalized disturbance τ_{dis} as in [15].

A. Structure analysis of disturbance attenuation

In complex domain, the output q of the actual plant $P(s)$ can be expressed from Fig. 2 as follows:

$$q = P \left[\frac{P_n}{\chi} (\tau_n + \tau_v) - \frac{P_n(1-Q)}{\chi} \tau_d - \frac{Q}{\chi} \xi \right], \quad (16)$$

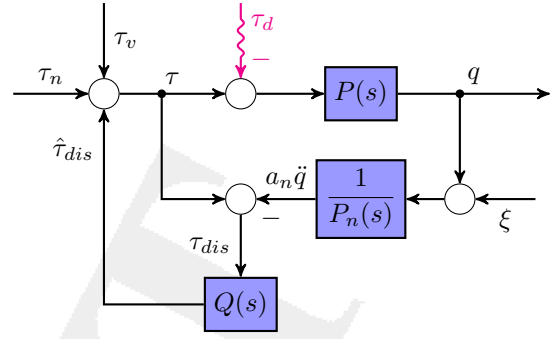


Fig. 2. System with additional feedback controls $\hat{\tau}_{dis}$ and τ_v

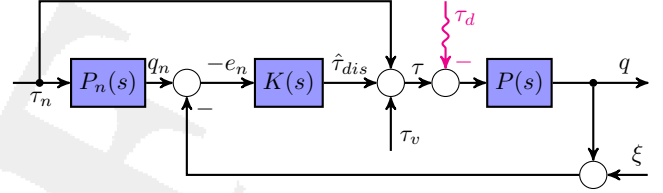


Fig. 3. Robust internal-loop compensator

where ξ is the measurement noise and $\chi(s) = P_n(s) + [P(s) - P_n(s)]Q(s)$. According to (16), below the cut-off frequency ω_c of the filter $Q(s)$ it should be arranged $|Q(j\omega)| \approx 1$ in order to compensate input disturbance τ_d . On the other hand, it should be achieved $|Q(j\omega)| \approx 0$ above the cut-off frequency of $Q(s)$, so the measurement noise ξ can be attenuated. Hence, the main goal is to make trade-off between $|1 - Q(j\omega)| \approx 0$ and $|Q(j\omega)| \approx 0$. The estimated disturbance $\hat{\tau}_{dis}$ can be reformulated using the RIC framework [1]–[5]:

$$\hat{\tau}_{dis} = -K(s)e_n. \quad (17)$$

Here $K(s)$ denotes the feedback compensator which needs to enforce plant $P(s)$ with disturbances τ_{dis} behave like a nominal model $P_n(s)$. The following error $e_n(t, q) = q(t) - q_n(t)$ represents the difference between the actual output q and the nominal output q_n . Fig. 2 can be equivalently transformed into Fig. 3 using the following parametrization (as in [2]):

$$Q(s) = \frac{P_n(s)K(s)}{1 + P_n(s)K(s)}. \quad (18)$$

Now, thanks to the parametrization of Q into P_n and K , systematic design of the filter Q is possible in the RIC framework using (18). For example, if the nominal system is chosen as a simple double integrator with nominal inertia, i.e. $P_n(s) = (a_n s^2)^{-1}$, then a derivative controller $K(s) = a_n \lambda s$ can be managed in order to achieve a linear low-pass filter:

$$Q(s) = \frac{\lambda}{s + \lambda}, \quad (19)$$

where λ is a positive coefficient representing the cut-off frequency of the linear filter (19).

B. Analysis of robust stability

For the system (13), let us consider a Lyapunov candidate as the positive definite function:

$$V = \frac{\sigma^2}{2}, V(0) = 0. \quad (20)$$

The first order time derivative of (20):

$$\dot{V} = \sigma \dot{\sigma}, \quad (21)$$

depends on the generalized error dynamics:

$$\dot{\sigma} = \ddot{q} - \left(\ddot{q}_{ref} - 2\Lambda \dot{e} - \Lambda^2 e \right) \quad (22)$$

$$= a_n^{-1} (\tau_n^{eq} + \tau_v + \hat{\tau}_{dis} - \tau_{dis}) - a_n^{-1} \tau_n^{eq} \quad (23)$$

$$= a_n^{-1} (\tau_v + \hat{\tau}_{dis} - \tau_{dis}). \quad (24)$$

The first derivative of V along the trajectories of the system (13) is computed using (21) and (24):

$$\dot{V} = a_n^{-1} \sigma (\tau_v + \hat{\tau}_{dis} - \tau_{dis}) \quad (25)$$

$$= a_n^{-1} \sigma (\tau_v - p). \quad (26)$$

Due to the matching condition, the generalized disturbance τ_{dis} appears exactly at the same point on the right-hand side of (25) where the additional control terms τ_v and $\hat{\tau}_{dis}$ appear. Hence, if $\hat{\tau}_{dis}$ is managed to compensate the generalized disturbance τ_{dis} , it is possible to select τ_v in order to cancel the effect of the disturbance compensation error p on \dot{V} according to (26), so that $a_n^{-1} \sigma (\tau_v - p) \leq 0$ is satisfied.

Assume that with the control input (12), the generalized disturbance τ_{dis} satisfies the inequality [15]:

$$|\tau_{dis}(t, q, \dot{q}, \tau)| \leq \rho(t, q, \dot{q}) + k |\tau_v(t, q, \dot{q}) + \hat{\tau}_{dis}(t, q, \dot{q})|, \quad (27)$$

where $\rho : [0, \infty) \times D \times D \rightarrow \mathbb{R}$ is a nonnegative continuous function and $k \in [0, 1)$ is a constant. The only information we need to know about the generalized disturbance τ_{dis} is the estimate (27). The function ρ represents a measure of the size of disturbances and uncertainties. It is not required ρ to be small, but only to be known. The goal is to show that with the knowledge of a function ρ , a coefficient k and Lyapunov function V , an additional controls $\hat{\tau}_{dis}$ and τ_v can be designed, so that the overall control (12) will stabilize the actual system (13) in the presence of internal and external disturbances. Right-hand side of (25) can be bounded as follows:

$$\dot{V} \leq a_n^{-1} (\sigma \hat{\tau}_{dis} + \sigma \tau_v + |\sigma| |\tau_{dis}|) \quad (28)$$

$$\leq a_n^{-1} (\sigma \hat{\tau}_{dis} + k |\sigma| |\hat{\tau}_{dis}|) + a_n^{-1} (\rho |\sigma| + \sigma \tau_v + k |\sigma| |\tau_v|). \quad (29)$$

We propose the generalized disturbance compensation $\hat{\tau}_{dis}$ and the additional control τ_v in the following form:

$$\hat{\tau}_{dis} = -\frac{\eta_1(t, q, \dot{q})}{1-k} \sigma, \quad (30)$$

$$\tau_v = -\frac{\eta_2(t, q, \dot{q})}{1-k} \text{sgn}(\sigma), \quad (31)$$

where $\eta_1(t, q, \dot{q})$ and $\eta_2(t, q, \dot{q})$ are nonnegative continuous functions for all $(t, q, \dot{q}) \in [0, \infty) \times D \times D$. The signs of

the additional control inputs (30) and (31) are opposite to the sign of the distance from the sliding manifold (6), thus directing the motion toward the equilibrium solution $\sigma = 0$. It follows from (29), (30) and (31):

$$\dot{V} \leq a_n^{-1} \left(-\frac{\eta_1}{1-k} \sigma^2 + k \frac{\eta_1}{1-k} |\sigma|^2 \right) + a_n^{-1} \left(\rho |\sigma| - \frac{\eta_2}{1-k} |\sigma| + k \frac{\eta_2}{1-k} |\sigma| \right) \quad (32)$$

$$= -a_n^{-1} \eta_1 \sigma^2 - a_n^{-1} \eta_2 |\sigma| + a_n^{-1} \rho |\sigma| \quad (33)$$

$$= -a_n^{-1} (1-\theta) \eta_1 \sigma^2 + a_n^{-1} (\rho - p_0 - \eta_1 \theta |\sigma|) |\sigma| - a_n^{-1} (\eta_2 - p_0) |\sigma| \quad (34)$$

$$\leq -a_n^{-1} (1-\theta) \eta_1 \sigma^2, \quad (35)$$

for all

$$\eta_1 \geq \frac{\rho - p_0}{\theta |\sigma|}, \quad \eta_2 \geq p_0, \quad (36)$$

where $\theta \in (0, 1)$ is constant parameter and p_0 is positive constant representing bounds of the disturbance estimation error p , namely $|p| \leq p_0$. The inequalities (35) and (36) ensure that the first order time derivative of V is negative definite and the trajectories of the closed-loop system (13) reach the positively invariant set:

$$\Omega_\eta = \left\{ |\sigma| \leq \frac{\rho - p_0}{\eta_1 \theta} \right\}, \quad (37)$$

in finite time and remain inside thereafter. Therefore, the solutions of the closed-loop system (13) are uniformly ultimately bounded. The term $a_n^{-1} \theta \eta_1 \sigma^2$ is added and subtracted on the right hand side of (34) in order to dominate over the only positive term $a_n^{-1} \rho |\sigma|$ outside the set (37). The radius of the ball (37) can be made arbitrarily small by increasing the magnitude η_1 of the additional control $\hat{\tau}_{dis}$. Therefore, the additional control terms (30) and (31) should be selected so the conditions (36) are satisfied. This means that the generalised disturbance τ_{dis} should be compensated by the magnitude η_1 of the disturbance attenuation based control term $\hat{\tau}_{dis}$, and the disturbance estimation error p caused by the disturbance compensator should be attenuated by the switching gain η_2 . It is important to notice that a sharper result could be obtained, if the magnitude η_2 of the switching control term τ_v is increased and selected to dominate over the whole generalised disturbance τ_{dis} , i.e. $\eta_2 \geq \rho$, but the chattering may be significant in this case. Namely, it could be derived using (34):

$$\dot{V} \leq -a_n^{-1} \eta_1 \sigma^2 + a_n^{-1} (\rho - \eta_2) |\sigma| \leq -a_n^{-1} \eta_1 \sigma^2, \quad (38)$$

for all $\eta_1 > 0$ and $\eta_2 \geq \rho$. The function \dot{V} is negative definite along the solutions of the closed-loop system (13), and the equilibrium point of the origin (6) is uniformly asymptotically stable.

III. APPLICATION TO THE HELICOPTER SYSTEM CE 150

A. Control strategy

The 2DOF helicopter system Humosoft CE 150 studied here is depicted in Fig. 4. It consists of the rigid body



Fig. 4. Laboratory helicopter system Humosoft CE 150

TABLE I
CONSTRAINTS FOR THE HELICOPTER INPUTS AND OUTPUTS

		Operational range
Inputs	u_1	[0, 0.6]
	u_2	[-0.3, 0.3]
	u_3	[-1, 0]
Outputs	ψ	[-45°, 45°]
	φ	[-130°, 130°]

with massive support, two propellers driven by DC motors, the power supply unit, the communication unit and the ballast. The helicopter body is driven with two DC motors with permanent stator magnets using pulse width modulation and power amplifiers. The helicopter position angles, the elevation and the azimuth, are measured by incremental encoders. In order to validate robustness properties of the control algorithm to the uncertainties and disturbances, the ballast is used in the real experiments to simulate dynamic changes in the center of gravity. Fig. 5 shows the overall control structure of the laboratory helicopter system. Three main parts are presented: the helicopter body, the PC based controllers and the interface module. The PC based controllers are designed in MATLAB (Simulink). The communication between the PC and the helicopter system is established by the multifunctional card MF624. It provides implementation of the control algorithms from the PC to the helicopter system and data acquisition from the helicopter system to PC. The real time experiments are performed using MATLAB xPC Target Toolbox.

B. Helicopter dynamics model

This subsection describes the summary mathematical model of the laboratory helicopter system CE 150 with two degrees of freedom, representing a highly nonlinear MIMO system with significant cross-couplings. The detailed modeling procedure is not in scope of this paper, therefore only the main results are depicted. The helicopter system has three inputs (voltage u_1 of the main motor, voltage u_2 of the tail motor and voltage u_3 of the servomotor for controlling the ballast position along the horizontal bar), and two outputs (the elevation angle ψ and the azimuth angle φ). Tab. I presents operating ranges of the helicopter input and output variables.

The elevation dynamics is described considering the torques in the vertical plane (depicted in Fig. 6) [12]:

$$a_\psi \ddot{\psi} = \tau_1 + \tau_\dot{\varphi} - \tau_{f_1} - \tau_m - \tau_G, \quad (39)$$

$$\tau_\dot{\varphi} = ml\dot{\varphi}^2 \sin \psi \cos \psi, \quad (40)$$

$$\tau_{f_1} = C_\psi \text{sgn} \dot{\psi} + B_\psi \dot{\psi}, \quad (41)$$

$$\tau_m = mgl \sin \psi, \quad (42)$$

$$\tau_G = k_G \dot{\varphi} \omega_1 \cos \psi, \quad (43)$$

for $\dot{\varphi} \ll \omega_1$. Here, a_ψ represents the moment of inertia around the horizontal axis, τ_1 is the moment produced by the main propeller, $\tau_\dot{\varphi}$ is the centrifugal torque, τ_{f_1} denotes Coulumb and viscous friction torques, τ_m is the gravitational torque, τ_G stands for the gyroscopic torque, m is the helicopter mass, g stands for the gravitational acceleration, l represents the distance from the vertical axis to the main motor axis, ω_1 denotes the angular velocity of the main propeller, k_G is the gyroscopic coefficient, B_ψ and C_ψ stand for viscous and Coulumb friction coefficients, respectively. Some influences are neglected in the elevation dynamics (39)–(43), such as motor stabilizing torque and variations of air resistance. This unmodeled dynamics should be compensated by the elevation disturbance observer.

The torques balance in the horizontal plane is computed to describe the azimuth dynamics [12]:

$$a_\varphi \ddot{\varphi} = \tau_2 - \tau_{f_2} - \tau_r, \quad (44)$$

$$\tau_{f_2} = C_\varphi \text{sgn} \dot{\varphi} + B_\varphi \dot{\varphi}, \quad (45)$$

$$a_\varphi = a_\psi \sin \psi, \quad (46)$$

where a_φ represents the inertia moment around the vertical axis, τ_2 denotes a moment produced by the tail propeller, τ_{f_2} stands for Coulumb and viscous friction torques, τ_r is a reaction torque of the main motor, ω_2 is the angular velocity of the tail propeller, B_φ and C_φ represent viscous and Coulumb friction coefficients. The azimuth disturbance observer should compensate unmodeled influences which are not considered through (44)–(46), such as coupling effects between the azimuth friction torque and the tail propeller speed.

C. The empirical model of the main DC motor and the main propeller dynamics

Since the body structure of the helicopter system CE 150 does not allow direct physical access to the appropriate internal signals, the main DC motor dynamics is approximated with the second order transfer function [12]:

$$\frac{\omega_1(s)}{u_1(s)} = \frac{1}{(T_1 s + 1)^2}. \quad (47)$$

Here, $\omega_1(s)$ and $u_1(s)$ stand for Laplace transforms of $\omega_1(t)$ and $u_1(t)$, respectively, and T_1 represent time constant of the main motor. The parabolic function of the angular velocity is used to approximately describe the main propeller torque [12]:

$$\tau_1(t) = a_1 \omega_1^2(t) + b_1 \omega_1(t), \quad (48)$$

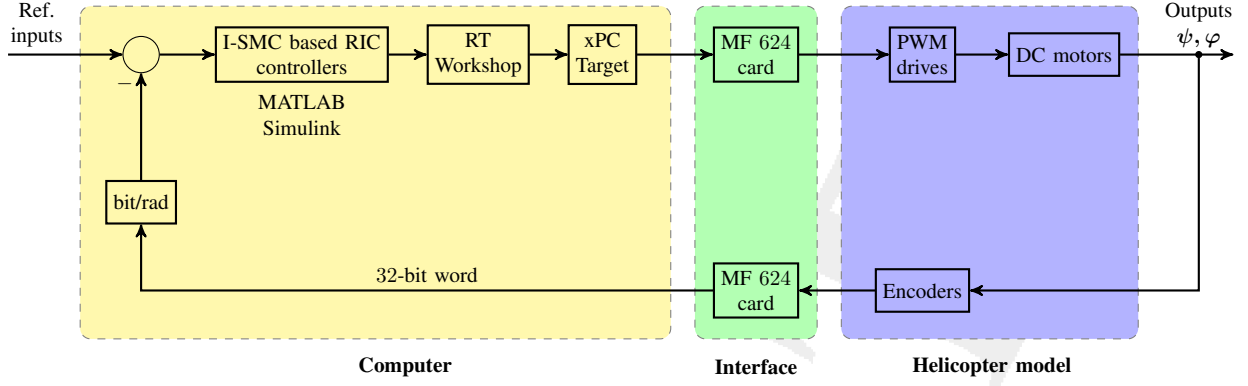


Fig. 5. Block diagram of the real-time control scheme for the helicopter system CE 150

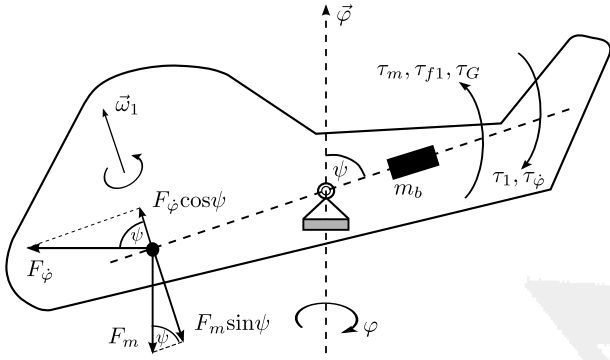


Fig. 6. Torques acting on the helicopter body in the vertical plane

where a_1 and b_1 denote parameters of the main propeller characteristic. Also, analogue relations to (47) and (48) are used to describe the tail DC motor dynamics with parameters T_2 , a_2 and b_2 .

D. The empirical model of the helicopter cross-coupling dynamics

One of the most composite features of the helicopter system CE 150 is strong cross-coupling effect between the elevation and azimuth dynamics. It is not possible to precisely identify these interaction torques, since no appropriate signal is available for measurement. Therefore, the reaction torque of the main motor to the azimuth dynamics is approximated with the first order transfer function [12]:

$$\frac{\tau_r(s)}{u_1(s)} = K \frac{T_z s + 1}{T_p s + 1}, \quad (49)$$

where T_z and T_p represent time constants, and K is a gain constant.

A simple genetic algorithm is used to identify all unknown helicopter parameters, which are listed in our previous paper [12].

E. Control Design

The elevation dynamics (39)–(43) can be specified with (2), introducing identities: $a_n \equiv a_\psi$, $q \equiv \psi$, $\tau_{dis} \equiv \tau_{f1} +$

$\tau_m + \tau_G - \tau_\phi$ and $\tau \equiv \tau_1$. Also, the azimuth dynamics (44)–(46) can be described with (2), using the substitutions: $a_n \equiv a_\varphi$, $q \equiv \varphi$, $\tau_{dis} \equiv \tau_{f2} + \tau_r$ and $\tau \equiv \tau_2$.

The helicopter system CE 150 is treated as decoupled set of two SISO systems, since the control algorithm is designed for a class of SISO nonlinear systems. Substituting $\eta_1 = a_n \lambda_1$, $\eta_2 = a_n \lambda_2$ and $k = 0$ in (30) and (31), the overall control for the helicopter system is derived in the vector form:

$$\tau = a_n \left(\ddot{q}_{ref} - 2\Lambda \dot{e} - \Lambda^2 e \right) - a_n \lambda_1 \sigma - a_n \lambda_2 \operatorname{sgn}(\sigma), \quad (50)$$

where $a_n = \operatorname{diag}(a_{n_\psi}, a_{n_\varphi})$, $q_{ref} = [q_{ref_\psi}, q_{ref_\varphi}]^T$, $\Lambda = \operatorname{diag}(\Lambda_\psi, \Lambda_\varphi)$, $e = [e_\psi, e_\varphi]^T$, $\lambda_1 = \operatorname{diag}(\lambda_{1_\psi}, \lambda_{1_\varphi})$, $\lambda_2 = \operatorname{diag}(\lambda_{2_\psi}, \lambda_{2_\varphi})$, $\sigma = [\sigma_\psi, \sigma_\varphi]^T$ and $\tau = [\tau_1, \tau_2]^T$. The disturbance attenuation control term $\hat{\tau}_{dis} = -a_n \lambda_1 \sigma$ of the overall control (50) is equivalent to the RIC based control (17) described with the transfer function $K(s) = a_n \lambda_1 s$ and the model following error $e_n = s^{-1} \sigma$. Thus, differently from conventional DOB based SMC [13], [14], the disturbance compensation is managed using the structural characteristics of the RIC and the closed-loop stability analysis is performed using the Lyapunov redesign framework. In comparison to the RIC based control schemes [1]–[5], the proposed algorithm has the potential to improve tracking performances and robustness properties to the disturbance compensation error p using the magnitude η_2 of the sliding mode control term τ_v .

Implementation of the control law (50) is depicted in Fig. 7. It consists of the feed-forward control term $\tau_{ff} = a_n \ddot{q}_{ref}$ to improve transient performances, the proportional-derivative feedback control term $\tau_{fb} = -a_n (2\Lambda \dot{e} + \Lambda^2 e)$ to enhance stability, the RIC based control term $\hat{\tau}_{dis} = -a_n \lambda_1 \sigma$ to attenuate the plant input generalized disturbance τ_{dis} , and the I-SMC based term $\tau_v = -a_n \lambda_2 \operatorname{sgn}(\sigma)$ to achieve robustness to the disturbance compensation error p . The gains λ_{1_ψ} and λ_{1_φ} need to be selected large enough, so they could extend the bandwidth of the closed-loop system and (36) could be satisfied.

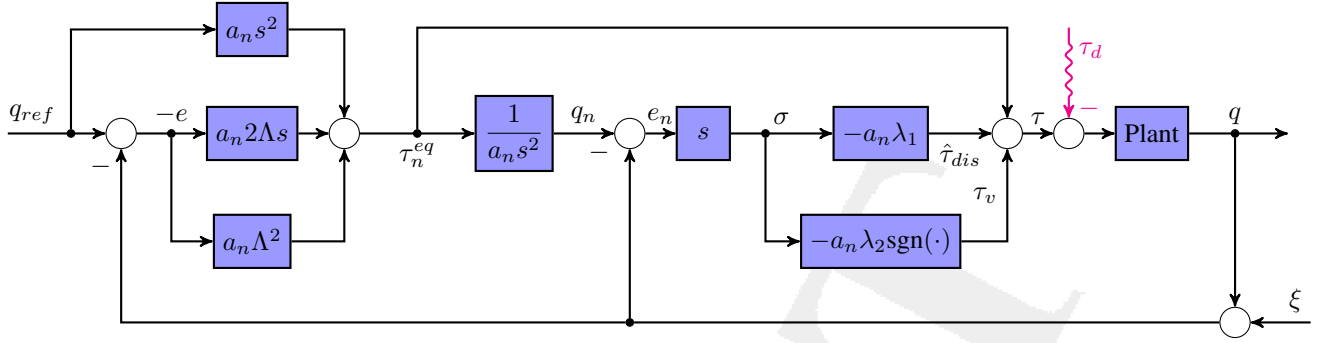


Fig. 7. I-SMC combined with the RIC for a class of nonlinear systems with matched uncertainties

IV. SIMULATION AND EXPERIMENTAL RESULTS

The DOB based SMC algorithm [13] exhibited most promising tracking performances and disturbance attenuation characteristics over the other control algorithms [9], [12], [13] implemented to the helicopter system CE 150. This section presents enhancement of the developed control method and results comparison with the DOB based SMC [13]. Although various reference signals are tested, the simultaneous steps in the reference inputs are selected due to the performance comparison with the control algorithms [9], [12], [13]. The perturbation tests are performed in the simulations and during the real experiments in order to investigate robustness properties of the proposed control scheme to the additional internal and external disturbances. All results are depicted for the following values of the controller parameters: $\Lambda = \text{diag}(3.5, 5.5)$, $\lambda_1 = \text{diag}(0.4, 0.7)$ and $\lambda_2 = \text{diag}(4, 4)$, which are not tuned for the best tracking performance, but rather to demonstrate the effective robustness properties of the proposed control method.

A. Simulation results

The simulation model of the helicopter system CE 150 has been developed in MATLAB (Simulink) according to the Section III. There are 30% uncertainties on the model parameters included in the simulation mode. Also, wind gusts with significantly strong magnitude (speed) of 10 m/s are represented by the sinusoidal signals (with high-frequency 50 rad/s and low-frequency 0.5 rad/s) and added to the helicopter dynamics. Angle responses of the elevation and azimuth dynamics are depicted in Fig. 8 and Fig. 9, respectively. It is notable that the RIC based I-SMC improved tracking performances in comparison with the DOB based SMC, especially when the limits of the helicopter outputs are approached. The RIC based I-SMC algorithm has provided excellent tracking performances over the entire range of the output variables, with lower overshoots and steady state errors.

B. Experimental results

The perturbation test is performed at the real experiment by changing the ballast position along its horizontal axis from the start to the end position. The ballast was at the middle

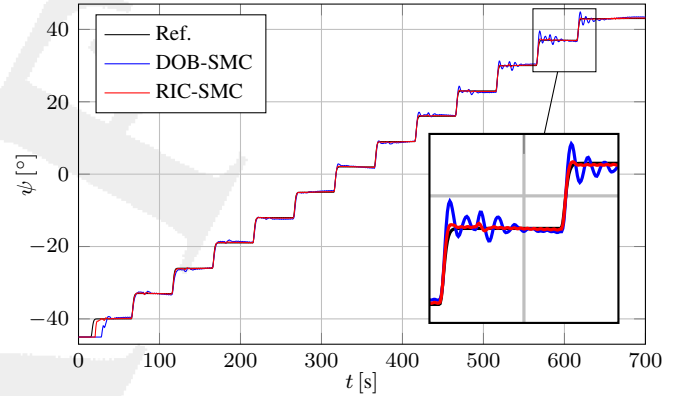


Fig. 8. Comparison of the elevation angle responses in the sim. mode

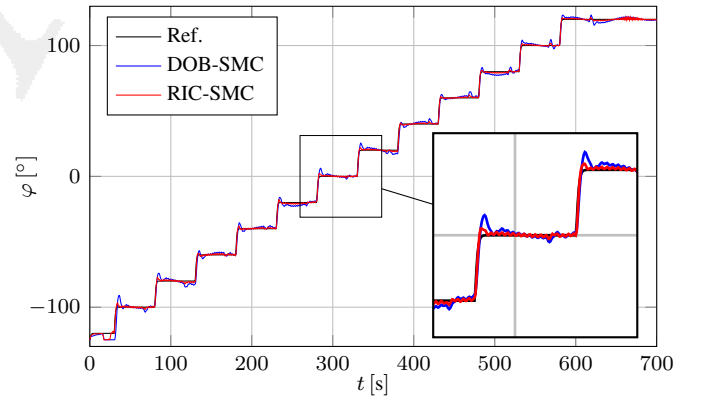


Fig. 9. Comparison of the azimuth angle responses in the sim. mode

position at the beginning of the test. The ballast motion was started about 160 second of the test, using the third control input presented in Fig. 12. The test results are depicted in Fig. 10, Fig. 11 and Fig. 12. In comparison with the DOB based SMC, the RIC based I-SMC provided superior tracking performances with lower tracking errors.

V. CONCLUSIONS

In this paper the synthesis of the I-SMC and the RIC is proposed for a class of nonlinear SISO systems with matched uncertainties. The designed control method introduces a gen-

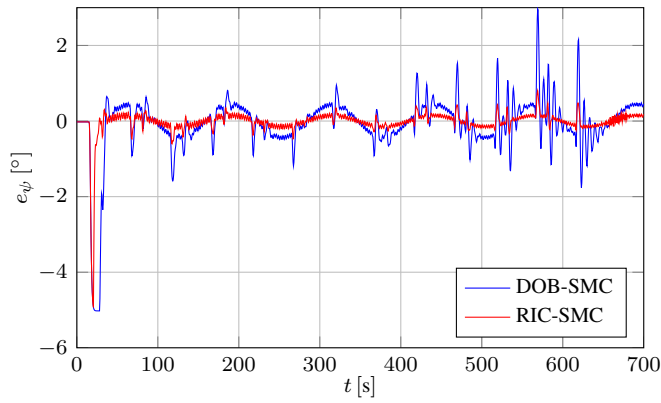


Fig. 10. Comparison of the elevation tracking errors at the real exp.

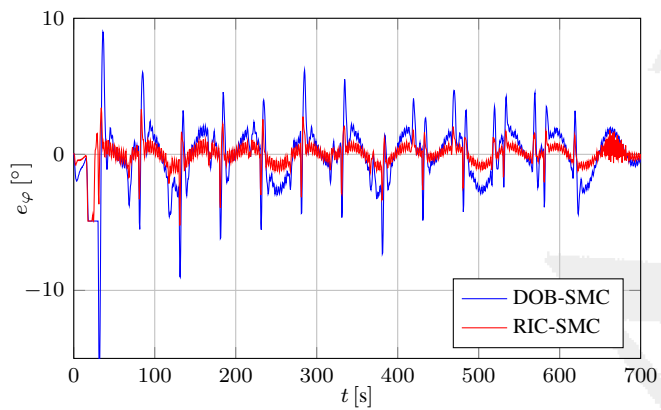


Fig. 11. Comparison of the azimuth tracking errors at the real exp.

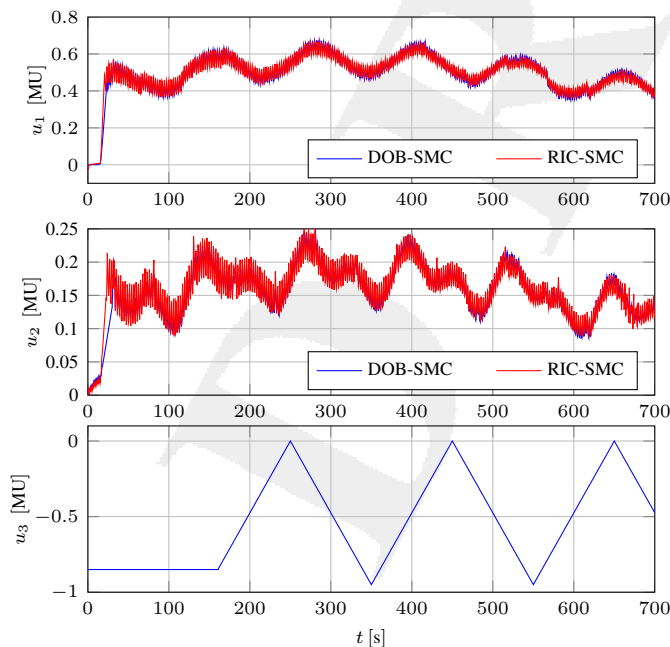


Fig. 12. Control inputs to the helicopter system

realisation of the well-known RIC based control for a class of linear systems. The RIC based I-SMC is implemented to the highly nonlinear small-scale helicopter system CE 150, demonstrating an excellent tracking performance and robust stability even in the presence of parametric uncertainties and external disturbances. Numerical simulations and real experiments have approved robustness properties of the developed control scheme under the perturbation test, that included ballast displacements, 30% uncertainties on the model parameters, and wind gusts with high amplitudes.

REFERENCES

- [1] B. K. Kim and W. K. Chung, "Performance predictable design of robust motion controllers for high-precision servo systems," in *American Control Conference, 2001. Proceedings of the 2001*, vol. 3, 2001, pp. 2249–2254 vol.3.
- [2] —, "Unified analysis and design of robust disturbance attenuation algorithms using inherent structural equivalence," in *American Control Conference, 2001. Proceedings of the 2001*, vol. 5, 2001, pp. 4046–4051 vol.5.
- [3] —, "Advanced design of disturbance observer for high performance motion control systems," in *American Control Conference, 2002. Proceedings of the 2002*, vol. 3, 2002, pp. 2112–2117.
- [4] —, "Performance tuning of robust motion controllers for high-accuracy positioning systems," *Mechatronics, IEEE/ASME Transactions on*, vol. 7, no. 4, pp. 500–514, Dec 2002.
- [5] B. K. Kim, W. K. Chung, and K. Ohba, "Design and performance tuning of sliding-mode controller for high-speed and high-accuracy positioning systems in disturbance observer framework," *Industrial Electronics, IEEE Transactions on*, vol. 56, no. 10, pp. 3798–3809, Oct 2009.
- [6] T. J. Koo and S. Sastry, "Output tracking control design of a helicopter model based on approximate linearization," in *Proceedings of the 37th IEEE Conference on Decision and Control*, vol. 4, Dec. 1998, pp. 3635–3640.
- [7] H. L. Pei, Y. Hu, and Y. Wu, "Gain scheduling control of a small unmanned helicopter," in *IEEE International Conference on Control and Automation*, 2007, pp. 1168–1173.
- [8] R. Xu and U. Ozguner, "Sliding mode control of a quadrotor helicopter," in *Decision and Control, 2006 45th IEEE Conference on*, Dec 2006, pp. 4957–4962.
- [9] J. Velagić and N. Osmić, "Design and implementation of fuzzy logic controllers for helicopter elevation and azimuth controls," in *IEEE Conference on Control and Fault Tolerant Systems*, Nice, France, Oct 2010, pp. 311–316.
- [10] J. Velagić and N. Osmić, "Identification and control of 2dof nonlinear helicopter using intelligent methods," in *IEEE Conference on System, Man and Cybernetics*, Istanbul, Turkey, 2010, pp. 2267–2275.
- [11] J. Balderud and D. I. Wilson, "A comparison of optimal control strategies for a toy helicopter," in *Asian Control Conference*, Singapore, Sep 2002, pp. 1432 – 1437.
- [12] A. Salihbegovic, E. Sokic, N. Osmic, and M. Hebibovic, "High performance disturbance observer based control of the nonlinear 2dof helicopter system," in *Information, Communication and Automation Technologies (ICAT), 2013 XXIV International Symposium on*, 2013, pp. 1–7.
- [13] A. Salihbegovic and M. Hebibovic, "Attitude tracking of the small-scale helicopter system using disturbance observer based sliding mode control," in *Control Automation (MED), 2014 22st Mediterranean Conference on*, 2014, pp. 1578–1583.
- [14] A. Šabanović and K. Ohnishi, *Motion control systems*. Chichester, United Kingdom: Wiley & Sons, Ltd, 2011.
- [15] H. Khalil, *Nonlinear Systems*. Prentice Hall, Jan. 2002.